ELSEVIER

Ceramics International 28 (2002) 99–103

CERAMICS INTERNATIONAL

www.elsevier.com/locate/ceramint

Electrical properties of sintered $Zr(RPO_4)_2 \cdot nH_2O$ (R = Li, Na, K, Rb and Cs) in a humid atmosphere

Susumu Nakayama*

Department of Applied Chemistry and Biotechnology, Niihama National College of Technology, Niihama 792-8580, Japan

Received 14 May 2001; received in revised form 13 June 2001; accepted 18 July 2001

Abstract

Five humidity sensor elements using porous ceramics prepared by sintered $Zr(RPO_4)_2 \cdot nH_2O$ (R = Li, Na, K, Rb and Cs) at 1000 °C were produced and the effect of microstructure on the humidity sensitivity was investigated. A layered structure was retained for the sintered samples (R = Na, K, Rb and Cs). For sintered $Zr(RPO_4)_2 \cdot nH_2O$ (R = Na, K, Rb and Cs), the impedance in the low-humidity region was about 1×10^8 Ω·cm and changed about four orders in the humidity region of 0–90% RH. The response time of sintered $Zr(RPO_4)_2 \cdot nH_2O$ (R = Li, K, Rb and Cs) for humidity change was about three minutes with a quick change of humidity from 60 to 90% RH and vice versa. Change in humidity sensitivity for all the sintered $Zr(RPO_4)_2 \cdot nH_2O$ samples was less than 5% RH for 200 days in room conditions.

Keywords: B. Microstructure-final; C. Electrical properties; C. Impedance; E. Sensors

1. Introduction

Humidity measurement and control is very important for a number of manufacturing and technological processes. Therefore, many types of humidity sensors have been investigated [1–9]. In humidity sensors using insulating porous ceramics without any mobile charge carriers, the admittance is usually enhanced by the formation of a physisorbed water layer (acting as a conductive path) on particle surfaces. The self-dissociated protons of physisorbed water act as a main charge carrier there migrating by hopping and/or Grotthuss-type transport processes on the particle surfaces. Therefore, the impedance in a humid atmosphere is characterized by the coverage of physisorbed water and the surface area and/or the microstructure of porous ceramics [1,2,6,7,10]. The addition of small amounts of a mobile cation such as H^+, Li^+, Na^+, or K^+ into a porous metal oxide [2–5,9] and the formation of a porous super-ionic conductor [11] can greatly improve the humidity sensitivity over the range of relative humidity. It has been reported that sintered $Zr(LiPO_4)_2 \cdot nH_2O$ is a very stable ionic conductor and any apparent changes in the resistivity and in its activation energy were not induced by immersion in water for 1 h [12–14]. It seems that sintered porous ceramics are a preferable material for the resistance type humidity sensor.

In this work the results obtained on electrical properties in a humid atmosphere of sintered $Zr(RPO_4)_2 \cdot nH_2O$ (R = Li, Na, K, Rb and Cs) are presented.

2. Experimental

Crystalline α-$Zr(HPO_4)_2 \cdot H_2O$ with a layered structure was prepared by adding phosphoric acid to zirconium fluorate solution in a bubbling stream of N_2 gas. The alkali salt, obtained by a convenient ion exchange method [15], was washed with distilled and deionized water and dried at 60 °C. The powder was pressed at 200 MPa into a plate, 6×6 mm wide and 0.5 mm thick and sintered at 60 °C for 2 h in air. Gold electrodes 4×4 mm (electrode area) were applied to both faces of the plate by vacuum evaporation (sandwich type element). The sintered $Zr(RPO_4)_2 \cdot nH_2O$ (R = Li, Na, K, Rb and Cs) samples were referred to as ZP–R (R = Li, Na, K, Rb and Cs).

The crystalline phase was identified at room temperature by powder X-ray diffraction technique (XRD). The

* Tel.: +81-897-37-7786; fax: +81-897-37-7842.
E-mail address: nakayama@chem.niihama-nct.ac.jp

0272-8842/02/$22.00
PII: S0272-8842(01)00063-3

microstructure was examined by scanning electron microscopy (SEM) and the pore size distribution was measured by mercury penetration porosimetry. The specific surface area was determined by the BET method using N_2 gas as a sorbate. Humidity-impedance characteristic was measured with an impedance meter (YHP 4192A) at 1 kHz. The frequency in a Cole–Cole plot measured at frequencies of 5 Hz to 13 MHz was nearly zero. Humidity (%RH) conditions, ranging from 0 to 90, were prepared by mixing dry and moist air in controlled proportions in the temperature range 30–45 °C.

3. Results and discussion

The XRD patterns are shown in Fig. 1. Except for ZP–Li, the peaks (d = 0.700–1.000 nm), corresponding to the interlayer distance, were confirmed. The d-values confirmed for ZP–R (R = Na, K, Rb and Cs) were consistent with the interlayer distance for anhydrous crystalline $Zr(RPO_4)_2 \cdot nH_2O$ (R = Na, K, Rb and Cs) completely exchanged with a monovalent cation. The layered structure was retained even after sintering to 1000 °C for ZP–R (R = Na,K,Rb and Cs) [13].

Fig. 2 shows the SEM photographs of α-$Zr(RPO_4)_2 \cdot H_2O$ and ZP–R (R = Li, Na, K, Rb and Cs). The appearances of $Zr(RPO_4)_2 \cdot nH_2O$ (R = Li, Na, K, Rb and Cs) dried at 60 °C were almost similar to that of α-$Zr(HPO_4)_2 \cdot H_2O$. For ZP–Li, the layered structure was decomposed and new small crystals appeared. For ZP–Na and ZP–K, traces of partial melting were confirmed, while each crystal retained a layered structure. Furthermore, no distinct variation in the external appearance of ZP–Rb was confirmed and the crystallinity of ZP–Cs increased [13,14].

The pore-size distributions of ZP–R are shown in Fig. 3. The pore volume and the surface areas for each ZP–R are summarized in Table 1. The pore volume of ZP–Li and ZP–Na was less than that of ZP–K, ZP–Rb and ZP–Cs. The cumulative volume of pores below 10 nm in radius for ZP–Na was more than other ZP–R. The surface area of ZP–Li was smaller than that of other ZP–R.

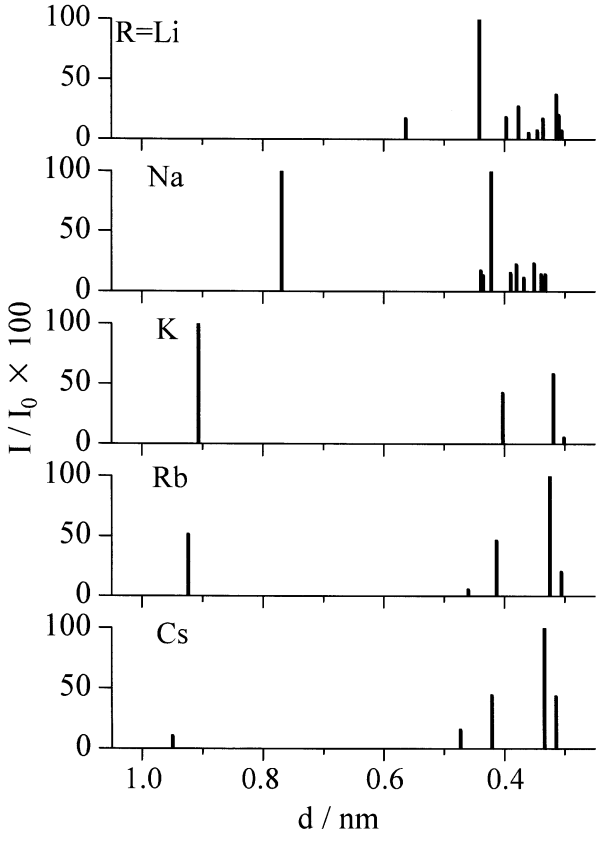

Fig. 1. XRD patterns of the sintered $Zr(RPO_4)_2 \cdot nH_2O$ <ZP–R>.

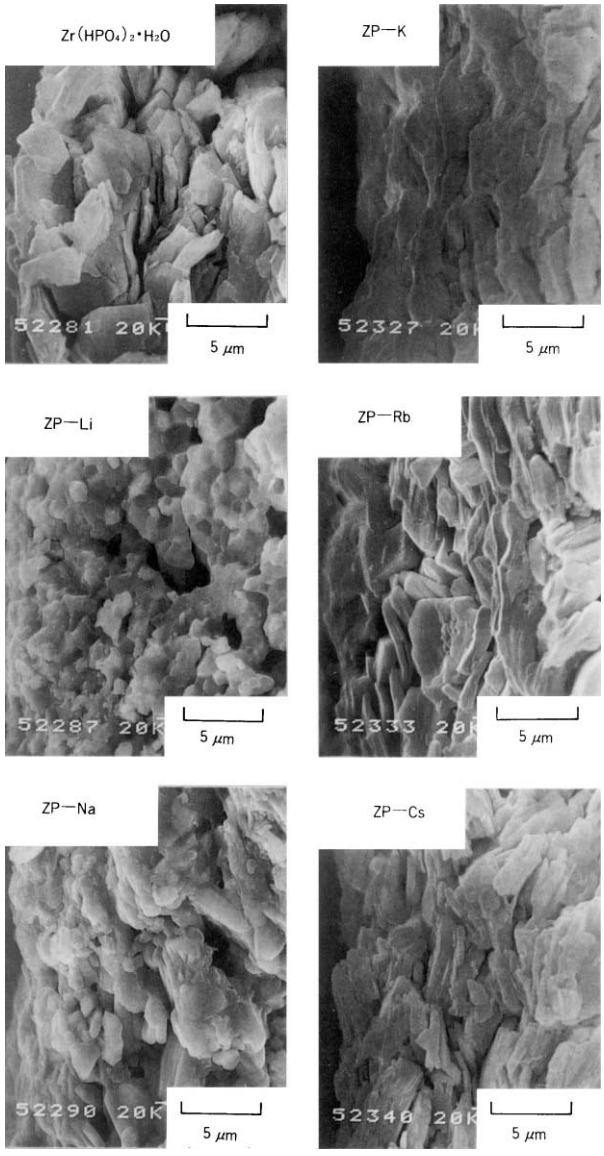

Fig. 2. Scanning electron micrographs of $Zr(HPO_4)_2 \cdot H_2O$ and the sintered $Zr(RPO_4)_2 \cdot nH_2O$ <ZP–R>.

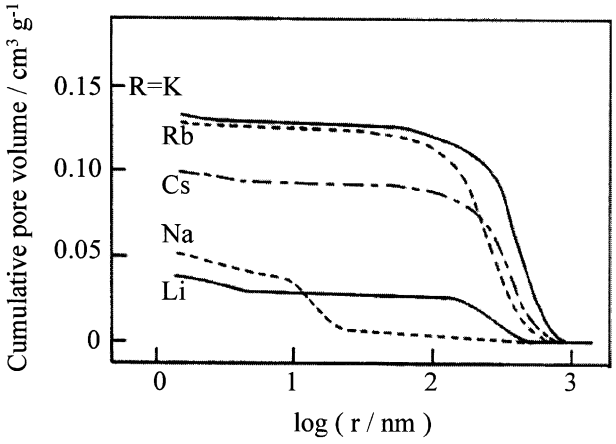

Fig. 3. Pore radius dependence of pore volume for the sintered $Zr(RPO_4)_2 \cdot nH_2O$.

Table 1
Characteristic values for the sintered $Zr(RPO_4)_2 \cdot nH_2O$ <ZP–R>

Sample name	Pore volume ($cm^3\ g^{-1}$)	Surface area ($\times 10^4\ cm^2\ cm^{-3}$)
ZP–Li	0.038	1.2
ZP–Na	0.052	5.4
ZP–K	0.132	7.3
ZP–Rb	0.128	5.2
ZP–Cs	0.098	7.8

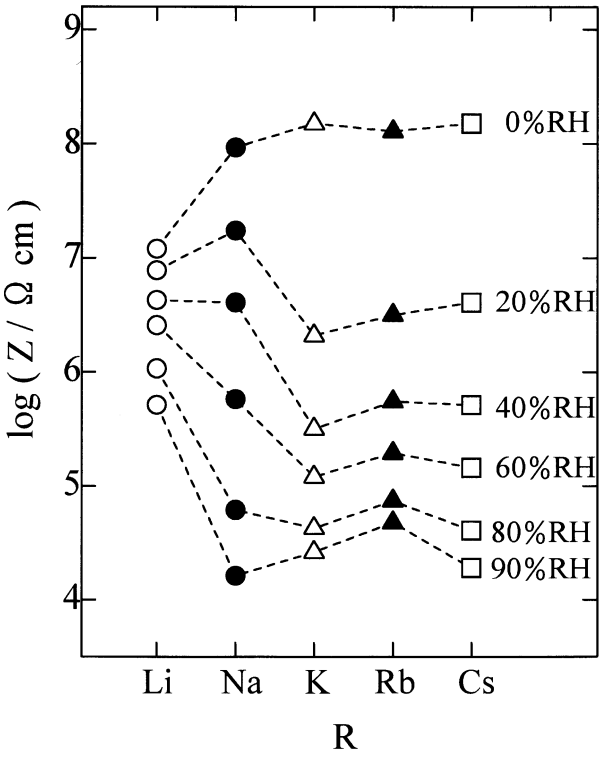

Fig. 4. Relationship between impedance and R of the sintered $Zr(RPO_4)_2 \cdot nH_2O$ system at an applied frequency of 1 kHz, 30 °C and several humidities.

Fig. 4 shows the humidity-impedance characteristics for ZP–R. The characteristics were different between ZP–Li and other ZP–R. The impedance of ZP–Li at 0% RH was 1.1×10^7 Ω•cm and changed only one order in the humidity region of 0–90% RH. On the other hand, the impedance of other ZP–R at 0% RH was about 1×10^8 Ω•cm and decreased four orders of magnitude by humidification to 90% RH. In the region of 20–60% RH, the impedance of ZP–Na was about one order of magnitude higher than those of ZP–K, ZP–Rb and ZP–Cs.

Fig. 5 shows the relationship between impedance at 90% RH and surface area. It has been reported that the slope (shown with broken line in Fig. 5) in the relationship between log (impedance) at 90% RH and log (surface area) is −1 for insulating porous ceramics (Al_2O_3, $ZrSiO_4$ etc.) [16]. For ZP–R (R = Na, K, Rb and Cs), the relationship between log (impedance) at 90% RH and log (surface area) was greatly located in the bottom from the broken line. It is understood that the impedances of ZP–R (R = Na, K, Rb and Cs) are lower than those of the insulating porous ceramics in spite of the small surface area of ZP–R. Similar tendencies are confirmed for the porous ceramics $Na_2Zr_2SiP_2O_{12}$ [11] and $LiAlSiO_4$ [17]. On the other hand, the result obtained for ZP–Li agreed with the relationship obtained for insulating porous ceramics without any mobile charge carriers.

The impedance responses for humidity changes from 60 to 90% RH and vice versa are shown in Fig. 6. By

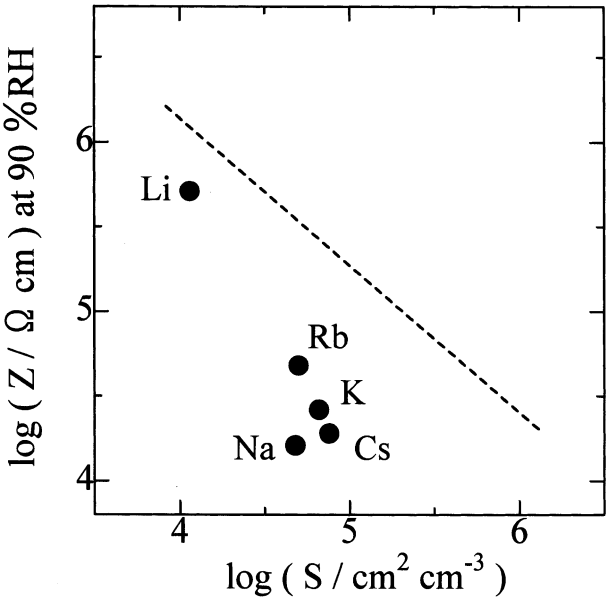

Fig. 5. Relationship between impedance at 90% RH and surface area for the sintered $Zr(RPO_4)_2 \cdot nH_2O$. - - - -: the insulating porous ceramics without any mobile charge carriers (Al_2O_3, $ZrSiO_4$ etc.).

using the method of mixing dry and moist air, a steady state in humidity is obtained within 3 min after setting. A steady state in the impedance of ZP–R (R = Li, K, Rb and Cs), except for ZP–Na, almost responded within three minutes after setting. The response time of ZP–Na

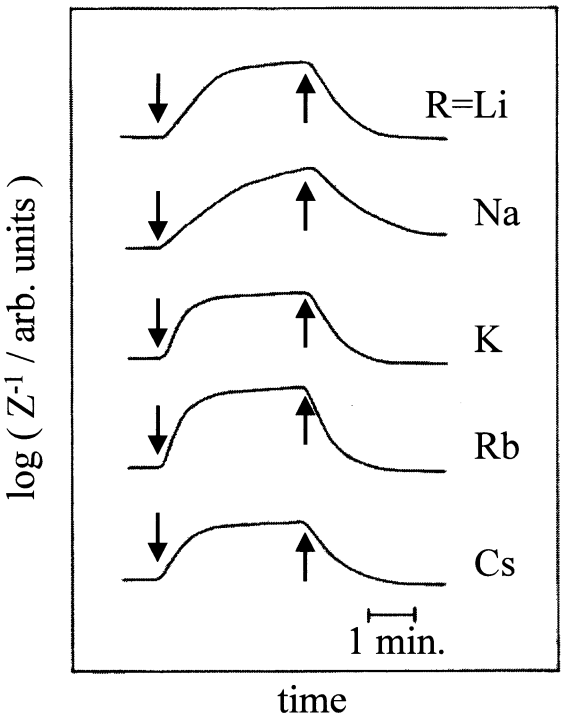

Fig. 6. Impedance response for humidity changes from 60 to 90% RH and vice versa for the sintered $Zr(RPO_4)_2 \cdot nH_2O$. (↓) 60% RH → 90% RH, (↑) 90% RH → 60% RH.

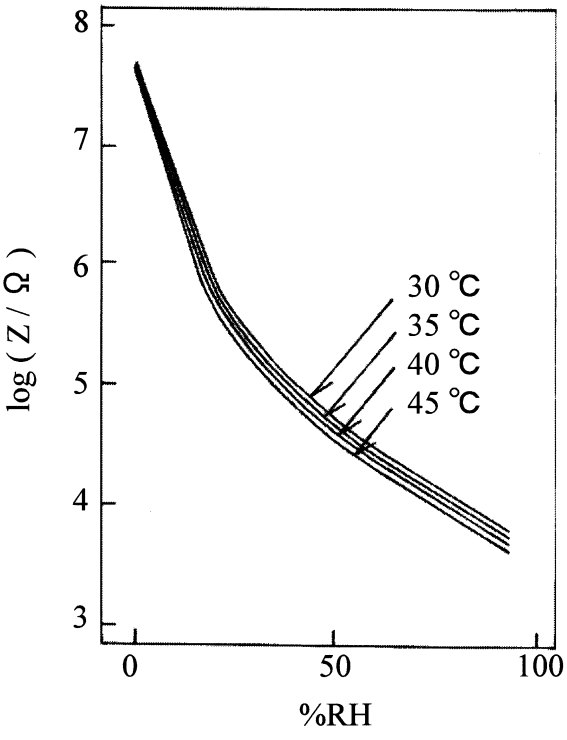

Fig. 7. Humidity dependence of impedance for the sintered $Zr(KPO_4)_2 \cdot nH_2O$ at an applied frequency of 1 kHz and several temperatures.

was considerably longer than those of other ZP–R. Similar tendencies were confirmed in the whole humidity region for all samples. The reason for the prolong response time for ZP–Na is considered to be that the volume fraction of pores smaller than 10 nm is larger than that of others.

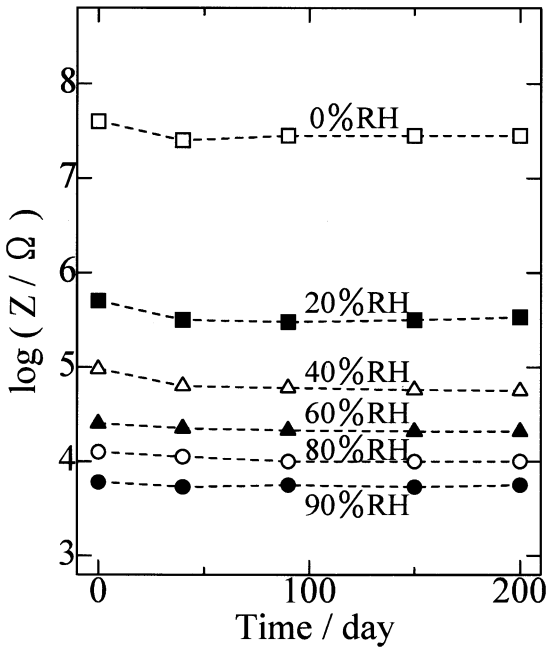

Fig. 8. Impedance changes for the sintered $Zr(KPO_4)_2 \cdot nH_2O$ after storage in room conditions.

The humidity-impedance characteristics of ZP–K at several temperatures are shown in Fig. 7. The temperature coefficient of the humidity-impedance characteristic for ZP–K in the temperature region of 30–45 °C was −0.5% RH/°C at 60% RH. The temperature coefficient of ZP–Li and ZP–R (R = Na, Rb and Cs) was –1.5% RH/° and −0.5% RH/°C, respectively.

The durability for 200 days in room conditions is shown in Fig. 8 for the ZP–K sensor element. A change in sensitivity was observed in the initial periods, while the impedance approached a stable value after that. The impedance changes at 0, 20, 40, 60, 80 and 90% RH were less than 5% RH during 200 days. For other ZP–R, the long term stability were also confirmed.

4. Conclusions

Electrical properties in a humid atmosphere of sintered $Zr(RPO_4)_2 \cdot nH_2O$ (R = Li, Na, K, Rb and Cs) at 1000 °C were investigated. For sintered $Zr(RPO_4)_2 \cdot nH_2O$ (R = Na, K, Rb and Cs), the impedance in the low-humidity region was about 1×10^8 Ω•cm and changed about four orders in the humidity region of 0–90% RH. The response time of sintered $Zr(RPO_4)_2 \cdot nH_2O$ (R = Li, K, Rb and Cs) for humidity change was a few minutes. Detected relative humidity using all the sintered $Zr(RPO_4)_2 \cdot nH_2O$ was accurate within ±5% RH even after 200 days storage in laboratory air. From these

results, it is concluded that sintered $Zr(RPO_4)_2 \cdot nH_2O$ (R = K, Rb and Cs) is a preferable material for use as a humidity sensing element.

References

[1] T. Nitta, Z. Terada, S. Hayakawa, Humidity-sensitive electrical conduction of $MgCr_2O_4$–TiO_2 porous ceramics, J. Am. Ceram. Soc. 63 (1980) 295–300.

[2] Y. Yokomizo, S. Uno, M. Harata, H. Hiraki, K. Yuki, Microstructure and humidity-sensitive properties of $ZnCr_2O_4$–$LiZnVO_4$ ceramic sensors, Sensor and Actuators 4 (1983) 599–606.

[3] F. Uchikawa, K. Shimamoto, Time variability of surface ionic conduction on humidity-sensitive SiO_2 films, Am. Ceram. Soc. Bull. 64 (1985) 1137–1141.

[4] Y. Sadaoka, M. Matsuguchi, Y. Sakai, S. Mitsui, Electrical properties of α-zirconium phosphate and its alkali salts in a humid atmosphere, J. Mater. Sci. 23 (1988) 2666–2675.

[5] K. Katayama, K. Hasegawa, H. Osawa, T. Akiba, H. Yanagida, Effect of K_2HPO_4 addition on the humidity sensitivity of Nd_2O_5-doped TiO_2, Sensors and Materials 2 (1990) 57–66.

[6] C. Cantalini, M. Pelino, Microstructure and humidity-sensitive characteristics of α-Fe_2O_3 ceramic sensor, J. Am. Ceram. Soc. 75 (1992) 546–551.

[7] G. Gusmano, G. Montesperelli, P. Nunziante, E. Traversa, Microstructure and electrical properties of $MgAl_2O_4$ and $MgFe_2O_4$ spinel porous compacts for use in humidity sensors, Br. Ceram. Trans. 92 (1993) 104–108.

[8] M.A. Hassen, A.G. Clarke, M.A. Swetnam, R.V. Kumar, D.J. Fray, High temperature humidity monitoring using doped strontium cerate sensors, Sensor and Actuators B69 (2000) 138–143.

[9] G. Neri, A. Bonavita, S. Galvagno, C. Pace, S. Patane, A. Arena, Humidity sensing properties of Li-iron oxide based thin films, Sensor and Actuators B73 (2001) 89–94.

[10] J.H. Anderson, G.A. Parks, The electrical conductivity of silica gel in the presence of adsorbed water, J. Phys. Chem. 72 (1968) 3662–3668.

[11] Y. Sadaoka, Y. Sakai, Humidity sensor using porous NASICON, Denki-kagaku 53 (1985) 395–399.

[12] J. Wang, I.D. Raistrick, R.A. Huggins, Preparation and conductivity of the layered structure j-phase of anhydrous crystalline $Li_2Zr(PO_4)_2$, J. Electrochem. Soc. 136 (1989) 2529–2532.

[13] Y. Sadaoka, M. Matsuguchi, Y. Sakai, S. Mitsui, M. Toita, K. Hatanaka, Effects of firing temperature on morphology and crystal structure of zirconium bis (monohydrogen phosphate) and its alkali salts, J. Mater. Sci. 24 (1989) 432–438.

[14] S. Nakayama, K. Itoh, S. Kakita, T. Suzuki, M. Sakamoto, Electrical properties of lithium phosphate ceramics prepared from $ZrLi_XH_{1-X}P_2O_8 \cdot nH_2O$, Ceram. Int. 25 (1999) 197–200.

[15] A. Clearfield, D.A. Tuhtar, On the mechanism of ion exchange in zirconium phosphates. 15. The effect of crystallinity of the exchanger on Li^+/H^+ exchange of α-zirconium phosphate, J. Phys. Chem. 80 (1976) 1296–1301.

[16] Y. Sadaoka, Y. Sakai, Humidity sensor using sintered alumina and zircon relation between electrical resistivity and surface area of the oxides, Denki-kagaku 51 (1983) 879–883.

[17] S. Nakayama, H. Kuroshima, Y. Sadaoka, Y. Sakai, Humidity sensor using porous ceramics $xLi_2O \cdot Al_2O_3 \cdot 2SiO_2$, J. Ceram. Soc. Jpn. 100 (1992) 968–971.